Self-Consistent Charge Equilibration Method and Its Application to $Au_{13}Na_n$ ($n = 1,10$) Clusters

Min Zhang[†] **and René Fournier***[,‡]

Department of Physics & Astronomy, and Department of Chemistry, York University, Toronto, Ontario, Canada M3J 1P3

Received: July 17, 2008; Revised Manuscript Received: November 28, 2008

We modified the charge equilibration method (QEq) of Rappé et al. by including the third and fourth order terms in the series expansion for the energy of charged atoms. This leads to a self-consistent scheme for obtaining charges and total energy in a molecule. We combined the modified QEq with a scaled morse potential (SMP) to get a new potential, SMP/QEq. The SMP/QEq method allows to do realistic geometry optimizations and calculate reliable charge distributions and ionization energies. The performance of SMP/QEq was fully tested by comparing to high level theories and experiments. We established a connection between first-principles DFT and SMP/QEq which gives insight into SMP/QEq and suggests ways to improve it.

I. Introduction

Potential functions play a determining role in any molecular simulation. It is important that a potential can estimate charge distribution correctly because not only electrostatic energy is a major part of the cohesive energy, but also charge distribution is crucial to understanding many physical properties, such as molecular reactivity. In the first application of the method that is described here, we showed that different and nontrivial types of AB ordering are possible in A_xB_{55-x} (A,B = Cu, Ag, Au) clusters depending on differences in electronegativity of the elements and the resulting charge transfer and electrostatic contributions to energy.[1] Many models have been proposed to describe charge distributions in molecules. Some models assign fixed charges to each atom, such as RESP.[2] However, a charge distribution model should depend on the molecular structures or else can treat only structures in close vicinity of the equilibrium geometries that are used to fit parameters of the model. Many methods were developed to estimate the charge distribution dynamically based on the electronegativity equalization principle of Sanderson.[3,4] Examples are the electronegativity equalization method (EEM),[5−8] chemical potential equalization (CPE),[9] and charge equilibration (QEq).[13] In this study, we modified Rappé's QEq method and combined it with the scaled morse potential (SMP).[1,12] We call this combination SMP/QEq and will explain it in some detail in section IV.

Initially, we implemented QEq based on Rappé's work,[13] but we got some physically unreasonable results. For example, for one of Ag_5Li_5 isomers in Figure 3, QEq assigns a charge bigger than +3 to a Li atom. Rappé et al. mentioned this problem and proposed to fix it by restricting charges to certain reasonable ranges. We believed that two factors contribute to this problem. First, in the original QEq method, the electronegativity χ and hardness η are those of the isolated atoms but they are applied to atoms-in-molecule (AIM).[29,30] We suggest instead to obtain a more suitable set of parameters by calculating χ and η for AIMs. Second, hardness represents an atom's ability to resist changes to its charge state. But if we charge an atom, both its electronegativity and hardness will change. As an extreme example, the hardness of Li^+ is clearly much larger than that of Li. So having a charge dependent hardness could prevent excessive charge build-up. Based on these two points, we developed the model described in the next section.

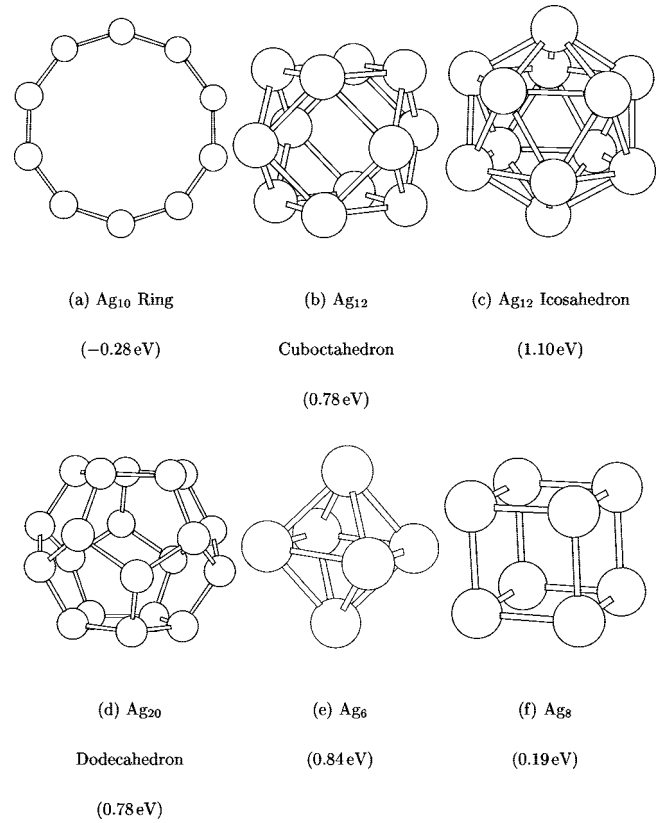

Figure 1. Special structures used for fitting. The difference between the first IE from QEq and SVWN, $IE_{QEq} - IE_{SVWN}$, are shown in parentheses.

II. Self-Consistent QEq Model

We formulate QEq by expanding atomic energy with respect to charge into a power series and retaining terms up to the fourth

* To whom correspondence should be addressed. E-mail: renef@yorku.ca.
† Department of Physics & Astronomy.
‡ Department of Chemistry.

10.1021/jp8063273 CCC: $40.75
Published on Web 03/06/2009

order instead of the second order as in the original implementation. All of the following discussions are about AIM unless specifically noted. We choose to cut at the fourth order term after trying a few models in the fitting procedure described in section III. This agrees with the suggestion from Iczkowski and Margrave.[16] So for atom i we have

$$E_i(Q_i) = E_i(0) + \chi_i^0 Q_i + \eta_i^0 Q_i^2 + \frac{1}{6}\left(\frac{\partial^3 E_i}{\partial Q_i^3}\right) Q_i^3 + \frac{1}{24}\left(\frac{\partial^4 E_i}{\partial Q_i^4}\right) Q_i^4 \quad (1)$$

Then by taking the sum of the charge induced energy on all atoms and adding the Coulomb interactions, we will have the total ionic energy of the entire molecule.

$$E(Q_1, ..., Q_N) = \sum_{i=1}^{N} [E_i(0) + \chi_i^0 Q_i + \eta_i^0 Q_i^2 + \frac{1}{6}\left(\frac{\partial^3 E_i}{\partial Q_i^3}\right) Q_i^3 + \frac{1}{24}\left(\frac{\partial^4 E_i}{\partial Q_i^4}\right) Q_i^4] + \sum_{\substack{i>j \\ i,j=1\cdots N}} J_{ij} Q_i Q_j \quad (2)$$

The derivation here is the same as the one in Rappé and Goddard's work.[13] If we take the first derivative of the total electrostatic energy with respect to Q_i, we have

$$\chi_i(Q_i) = \chi_i^0 + 2Q_i\lambda_i(Q_i) + \sum_{\substack{j\neq i \\ j=1\cdots N}} J_{ij} Q_j \quad (3)$$

where $\lambda_i(Q_i) = \eta_i^0 + {}^1/_4[(\partial^3 E_i)/(\partial Q_i^3)]Q_i + {}^1/_{12}[(\partial^4 E_i)/(\partial Q_i^4)]Q_i^2$ can be regarded as a charge-dependent hardness, J_{ij} stands for the screened Coulomb interaction, and $\chi_i(Q_i)$ is the electronegativity of atom i in the molecule. This modification of QEq requires an iterative calculation because of the nonlinear relation it brings. An iterative scheme was introduced in previous work[14,15] but only for the hydrogen atom.

The Sanderson's principle[3,4] states that only one global electronegativity exists in a N-atom system. Therefore, when atoms form a molecule, their electronegativities must equalize. For a N-atom system, we have

$$\chi_1 = \chi_2 = ... = \chi_N \quad (4)$$

We also know the total charge on a system

$$Q_{\text{total}} = \sum_{i=1}^{N} Q_i \quad (5)$$

By combining eqs 3−5, we have the linear system

$$\begin{bmatrix} J_{21}-J_{11} & J_{22}-J_{12} & J_{23}-J_{13} & ... & J_{2i}-J_{1i} & ... & J_{2N}-J_{1N} \\ J_{31}-J_{11} & J_{32}-J_{12} & J_{33}-J_{13} & ... & J_{3i}-J_{1i} & ... & J_{3N}-J_{1N} \\ \vdots & \vdots & \vdots & \vdots & \vdots & \vdots & \vdots \\ J_{i1}-J_{11} & J_{i2}-J_{12} & J_{i3}-J_{13} & ... & J_{ii}-J_{1i} & ... & J_{iN}-J_{1N} \\ \vdots & \vdots & \vdots & \vdots & \vdots & \vdots & \vdots \\ J_{N1}-J_{11} & J_{N2}-J_{12} & J_{N3}-J_{13} & ... & J_{Ni}-J_{1i} & ... & J_{NN}-J_{1N} \\ 1 & 1 & 1 & ... & 1 & ... & 1 \end{bmatrix} \times \begin{bmatrix} Q_1 \\ Q_2 \\ \vdots \\ Q_i \\ \vdots \\ Q_{N-1} \\ Q_N \end{bmatrix} = \begin{bmatrix} \chi_1^0 - \chi_2^0 \\ \chi_1^0 - \chi_3^0 \\ \vdots \\ \chi_1^0 - \chi_i^0 \\ \vdots \\ \chi_1^0 - \chi_N^0 \\ Q_{\text{total}} \end{bmatrix} \quad (6)$$

For J_{ij}, if $i \neq j$, we use the empirical function developed by Louwen and Vogt.[10]

$$J_{ij} = \left(\frac{1}{\gamma_{ij}^3} + R_{ij}^3\right)^{-1/3} \quad (7)$$

where $\gamma_{ij} = 2[\eta_i^0\eta_j^0]^{1/2}$.[11] When i is equal to j, we have $J_{ii} = 2\lambda_i(Q_i)$, which is a charge dependent parameter. In eqs 6 and 7, all quantities are in atomic units. To develop the linear system, we rewrite eq 4 to $N-1$ equations, $\chi_i - \chi_1 = 0$, where $i = 2,..., N$. This choice is arbitray and assigns a "special status" to atom 1 in the linear system. But this should not cause any problem when we apply the LU decomposition with partial pivoting and row interchanges to solve the linear system, and in practice, we have not encountered any case of numerical instability.

III. Fitting Procedure

The major difficulty in implementing this scheme is that the various energy derivatives in eq 1, including χ_i^0 and η_i^0, are unknown. We designed a fitting procedure to obtain them from a higher level theory, in the present work density functional theory (DFT) in the local spin density approximation with a "SVWN" exchange-correlation functional.[20−23] For fitting, we selected model structures in which all atoms are equivalent, as shown in Figure 1. The simplest one is a 10-atom ring. We found that when a ring contains more than 10 metal atoms DFT calculations are costly and very hard to convergence. On the other hand, smaller rings give less data for fitting and bigger error could arise due to atomic interactions between non-neighbor atoms that are closer to each other. Other high-symmetry structures can be used such as 12-atom cuboctahedron, 12-atom icosahedron, 20-atom dodecahedron, etc. We chose these high-symmetry structures because the partial charge on each atom can be simply calculated by $Q_i = Q_{\text{total}}/N$, so we do not have to choose among different charge decomposition schemes in ab initio calculations. Another benefit is that coefficients are always identical for all atoms in a model system and this simplifies our fitting procedure. The fitting procedure consists of the following steps. First, for a N-atom structure, we calculate the total energies with different charges, $E_{\text{total}}(Q_{\text{total}})$, where Q_{total} ranges from -1 to N, using SVWN/DFT and the deMon software.[33] Spin states were restricted to singlet or doublet. Model core potentials were used for Ag and Au, with 17 electrons per atom being treated explicitly. All electron treatments were done for the other elements. The basis sets were of double-ζ quality (except triple-ζ for K) with diffuse and

TABLE 1: Coefficients of the $E(Q)$ Polynomial Fit

element	first	second	third	fourth	χ	λ	2nd/λ
Li	3.0215	3.2426	0.9056	0.0566	3.01	2.39	1.357
Na	2.8815	3.1339	0.6762	−0.1326	2.85	2.30	1.362
K	2.4419	2.5684	0.5326	−0.0996	2.42	1.92	1.337
Rb	2.3138	2.4580	0.5036	−0.1247	2.33	1.85	1.329
Cu	5.2775	4.1921	0.3808	0.2151	4.48	3.25	1.290
Ag	5.1362	4.2742	0.4097	−0.0490	4.44	3.14	1.361
Au	6.3450	4.0789	0.1825	0.1245	5.77	3.46	1.179
Al	3.8002	2.7974	0.1283	0.7036	3.21	2.78	1.006

polarization functions for all elements except Ag and Au. The auxiliary basis sets were standard ones used in the deMon software.[33,34] From each calculation we can extract a pair of data, charge on each atom and corresponding atomic charge-induced energy, $(Q_i,E_i(Q_i))$. As mentioned earlier, Q_i is simply equal to Q_{total}/N due to symmetry. We get the AIM charging energy as

$$E_i(Q_i) = [E_{\text{total}}(Q_{\text{total}}) - E_{\text{total}}(0) - \sum_{\substack{m<n \\ m,n=1\cdots N}} J_{mn}Q_mQ_n]/N \tag{8}$$

The right-hand side of eq 8 could be interpreted as follows. we use the neutral system as the reference for energy and subtract it from the energy of the charged systems. The underlying assumption in eq 8 is that the nonionic terms in the energy are equal in the neutral and charged systems. Therefore, the energy difference between neutral and charged has two contributions: (i) the energy for charging atoms and (ii) the pairwise electrostatic interactions between atoms. After we subtract Coulomb energies, represented by the sum term in eq 8, we have only the energy for charging atoms left. Again because of symmetry we can obtain $E_i(Q_i)$ simply by dividing the total charge-induced energy by N. In fitting, we approximate J_{ij} by eq 7. In this procedure, we must choose sensible interatomic distances. After many trials we decided that the best choice is simply to set the nearest neighbor distance (d_{NN}) in the model system equal to d_{NN} of the corresponding bulk system. The fitting results from different model structures are not identical. We expect this difference since atoms in different model systems are in distinct molecular environment, strictly they are different AIMs, and this should be reflected in the parameters obtained. Ideally, we should choose parameters from model systems resembling the dominant cluster structures which are usually compact and have high coordination numbers. However, we compared the performance of SMP/QEq using different sets of coefficients, and found that those from the simplest model structure (10-atom ring) work the best. We elaborate on this point in section V.B. A possible reason is that in our fitting precedure we introduced a few approximations. The more complex a structure is, the bigger the error is from approximations due to the entanglement of its atomic interactions. The 10-atom ring has the simplest structure and the lowest coordination. The only negative point of a 10-atom ring is that it does not possess a compact structure typical of low energy clusters structures. This defect causes a systematic error that will be discussed in section V.D.

The coefficients we obtained with this fitting procedure for eight metals are listed in the first four columns of Table 1. Since we use neutral systems as reference for energy, as expected, the zeroth order coefficients are essentially zero. In the next two columns of the table, we list the electronegativity χ and hardness λ of isolated atoms from Parr and Yang's book,[17] which are counterparts to the first and second order coefficients. The last column contains the ratio of our hardness to theirs. We observe that for alkali we obtained almost the same electronegativity and bigger hardness. For group 11 elements, both electronegativity and hardness are bigger than Parr and Yang's values. For Al we obtained a bigger electronegativity but the same hardness. The second order coefficients are almost always bigger than those from Parr and Yang's book, meaning atoms in molecules are harder than the isolated ones. Consequently, unphysical big charges generated by using parameters for isolated atoms will be reduced if we apply those found for atoms in molecules. In addition, the third and fourth parameters give a more realistic description of systems with large atomic charges.

IV. Explanation of SMP/QEq by DFT

We now wish to review some aspects of DFT formalism[17] in order to show the assumptions that give rise to SMP/QEq and similar approximate methods.

Consider a N-electron system: if the external potential $v(r)$ is known, the Hamiltonian of the system is determined. Thus N and $v(r)$ determine all ground-state properties of the system. The derivatives of energy with respect to N and $v(r)$ are

$$\mu = \left(\frac{\partial E}{\partial N}\right)_v \tag{9}$$

$$\eta = \frac{1}{2}\left(\frac{\partial \mu}{\partial N}\right)_v = \frac{1}{2}\left(\frac{\partial^2 E}{\partial N^2}\right)_v \tag{10}$$

$$f(r) = \left(\frac{\delta \mu}{\delta v}\right)_N = \left(\frac{\partial \rho(r)}{\partial N}\right)_v \tag{11}$$

$$\rho(r) = \left[\frac{\delta E}{\delta v(r)}\right]_N \tag{12}$$

In these relations, μ is the chemical potential of the system, η is the absolute hardness, $f(r)$ is the Fukui function, and $\rho(r)$ is the ground-state electron density. With the help of these derivatives, we can do a Taylor expansion for the ground-state energy (see ref 17, page 226)

$$\Delta E = \mu^0\Delta N + \eta^0(\Delta N)^2 + \Delta N \int f^0(r)\Delta v(r)\,dr + \frac{1}{2}\int\int \left[\frac{\delta \rho^0(r)}{\delta v(r')}\right]_N \Delta v(r)\Delta v(r')\,dr\,dr' + \int \rho^0(r)\Delta v(r)\,dr \tag{13}$$

where we use superscript "0" to indicate quantities for the system before any changes. Since electronegativity χ is equal to $-\mu$ and charge Q is equal to $-\Delta N$, we can substitute variables in eq 13 and get

$$\Delta E = \chi^0 Q + \eta^0 Q^2 - Q \int f^0(r)\Delta v(r)\,dr + \frac{1}{2}\int\int \left[\frac{\delta \rho^0(r)}{\delta v(r')}\right]_N \Delta v(r)\Delta v(r')\,dr\,dr' + \int \rho^0(r)\Delta v(r)\,dr \tag{14}$$

If only the external potential $v(r)$ changes, the first, second, and third terms in eq 14 will be zero. If $v(r)$ is fixed and N varies, the fourth, fifth, and third terms will disappear. So

we can say, in regard to energy, that the first and second terms describe the effect of varying the number of electrons and the fourth and fifth terms tell us how changes of external potential induce energy variation. The third term shows the compound effect when both quantities are changed.

Let us consider our simplest model system, a 10-atom ring, Figure 1a. From the viewpoint of atom i, other atoms serve as particle source and additional external field. We use eq 14 to represent the energy change, ΔE_i, for atom i when forming a ring. If the ring is neutral, because all atoms are equivalent, every atom has a zero charge. This means terms 1, 2, and 3 will be zero. Because bonding changes $v_i(r_i)$, terms 4 and 5 will not be zero and their sum is ΔE_i. This is what SMP attempts to represent. That is, in SMP/QEq we use SMP[1,12] to approximate terms 4 and 5 in eq 14 due to nonionic interaction. The only conceptual difference is that SMP assigns energy to bonds, but terms 4 and 5 in eq 14 assign the same energy to atoms. Actually, other potentials, such as embedded-atom method (EAM)[31] and Morse potential,[32] can do the same thing. It is essential, however, that the chosen empirical potential be "purely covalent", i.e., that it does not attempt in any way to describe ionic or other electrostatic interactions. The SMP fits this criterion perfectly.

Now let us change the energy further by charging the ring while keeping its size fixed. χ^0 and η^0 were changed during ring formation. To avoid any ambiguity, we rewrite eq 14 as

$$\Delta E_i = \chi^0_{2i} Q_i + \eta^0_{2i} Q_i^2 - Q_i \int f^0_{2i}(r_i) \Delta v(r_i)\, \mathrm{d}r_i + \frac{1}{2} \int\int \left[\frac{\delta \rho^0_{2i}(r_i)}{\delta v_i(r_i')}\right]_N \Delta v(r_i) \Delta v(r_i')\, \mathrm{d}r_i\, \mathrm{d}r_i' + \int \rho^0_{2i}(r_i) \Delta v(r_i)\, \mathrm{d}r_i \quad (15)$$

The subscript 2 represents coordination number and serves as a reminder that the parameters refer to an AIM not an isolated atom. For atom i, ΔE_i comes from two sources, charge Q_i and $\Delta v_i(r_i)$ We need to make a few approximations to reach the main equation of QEq. First, we approximate $\Delta v_i(r_i)$ by the Coulomb field generated by charges on other atoms. We also accept the "frozen core" assumption. Under this assumption, when an atom gains negative charges, the only change to its density is that additional electron density is added to its lowest unoccupied molecular orbital (LUMO). Similarly, the only change to a positively charged atom is that the positive charge spreads in its highest occupied molecular orbital (HOMO). So we can approximate atom j's contribution to $\Delta v_i(r_i)$ as $g_j(r_i) = -Q_j \int (\rho_j(r_j))/(|r_j - r_i|)\, \mathrm{d}r_j$ where $\rho_j(r_j)$ is the density of the LUMO or HOMO of atom j, depending on the sign of Q_j Then we have $\Delta v_i(r_i) = \sum_{j \neq i} g_j(r_i)$. Usually, $f^0(r)$ is approximated using central difference as: $f^0(r) \approx {}^1/_2[\rho_{\mathrm{LUMO}}(r) + \rho_{\mathrm{HOMO}}(r)]$ [ref 17, p 99]. Here we choose a one-sided difference formula and get $f^0(r) \approx \rho_i(r_i)$, where $\rho_i(r_i)$ is the density of LUMO or HOMO depending on the sign of Q_j. We can rewrite the third term in eq 15 as

$$-Q_i \int f^0_{2i}(r_i) \Delta v(r_i)\, \mathrm{d}r_i \approx Q_i \sum_{j \neq i} \int\int \frac{Q_j \rho_i(r_i) \rho_j(r_j)}{|r_i - r_j|}\, \mathrm{d}r_i\, \mathrm{d}r_j = \sum_{\substack{j \neq i \\ j=1 \cdots N}} J_{ij} Q_i Q_j \quad (16)$$

Another approximation is that we neglect terms 4 and 5 in eq 15 if we believe that the disturbance to external field due to Coulomb field contributes little to energy change via terms 4 and 5 compared to other terms. Accepting this simplification, we in fact represent terms 4 and 5 by SMP completely. After all these approximations, we get the equation

$$\Delta E_i = \chi^0_{2i} Q_i + \eta^0_{2i} Q_i^2 + \sum_{\substack{j \neq i \\ j=1 \cdots N}} Q_i Q_j J_{ij} \quad (17)$$

ΔE_i represents the ionic energy of atom i if we treat other atoms as particle source and additional external field. This way of thinking makes us assign all of the Coulomb energy between atom i and all other atoms to atom i as potential energy. That is, considering atom i and j, when we write down eq 17 for atom i, the Coulomb energy between these two atoms is completely given to atom i. In eq 17 for atom j, we assign this energy to atom j. So when we sum ionic energies represented by eq 17 to get total ionic energy, we have to avoid double counting of Coulomb energies

$$\Delta E_{\mathrm{total}}(Q_1, ..., Q_N) = \sum_{i=1}^{N} (\chi^0_{n_i i} Q_i + \eta^0_{n_i i} Q_i^2) + \sum_{\substack{i>j \\ i,j=1 \cdots N}} Q_i Q_j J_{ij} \quad (18)$$

In eq 18, the subscript n_i represents the environment around atom i since eq 17 is true for any AIM. If we take the first derivative of $\Delta E_{\mathrm{total}}$ with respect to Q_i, we have the basic equation of QEq.[13] Adding higher order terms to the equation above will give

$$\chi_i(Q_i) = \chi^0_{n_i i} + 2 Q_i \lambda_{n_i i}(Q_i) + \sum_{\substack{j \neq i \\ j=1 \cdots N}} J_{ij} Q_j \quad (19)$$

where $\lambda_{n_i i}(Q_i) = \eta^0_{n_i i} + {}^1/_4[(\partial^3 E_i)/(\partial Q_i^3)]^0_{n_i} Q_i + {}^1/_{12}[(\partial^4 E_i)/(\partial Q_i^4)]^0_{n_i} Q_i^2$. This the basic equation in our version of QEq, eq 3. If we apply eq 19 to all of our model systems, the only difference is the subscripts representing molecular environment, n_i. That is to say, when we perform fitting using different model systems, we will get parameters for different AIMs.

V. Result

To test the performance of SMP/QEq, we did several calculations. Results are shown and discussed below.

A. Diatomic Molecules. Metal heterodimers are the simplest alloy systems. In this test, we calculated the bond length, R_e, and dissociation energy, D_e, for 15 heterodimers AB (A,B = Li, Na, K, Cu, Ag, and Au). Four different methods, SMP, SMP/QEq, SVWN, and BP86,[26,27] were used. Results are summarized in Figure 2. We use results from BP86 as a reference because it is theoretically the best method and also because it generally agrees with experiment better than SVWN. The other methods are compared to BP86. Figure 2b shows comparison for D_e. The points gathered around 0.6 eV are for LiNa, LiK, and NaK in which ionic interaction is weak since Li, Na, and K have similar electronegativities. In those three cases, SMP and SMP/QEq give almost the same values as SVWN and BP86, as

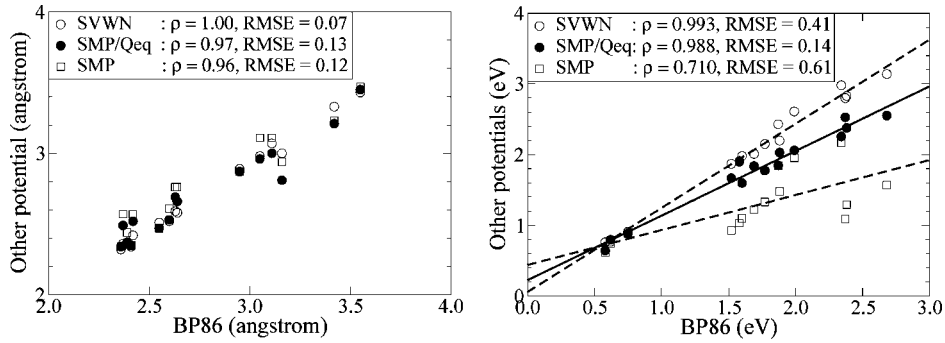

(a) Bond length (b) Dissociation energy

Figure 2. Dissociation energy and bond length of metal heterodimers calculated by four different methods, SMP, SMP/QEq, SVWN, and BP86; ρ and RMSE represent the correlation coefficient and root-mean-square-error, respectively.

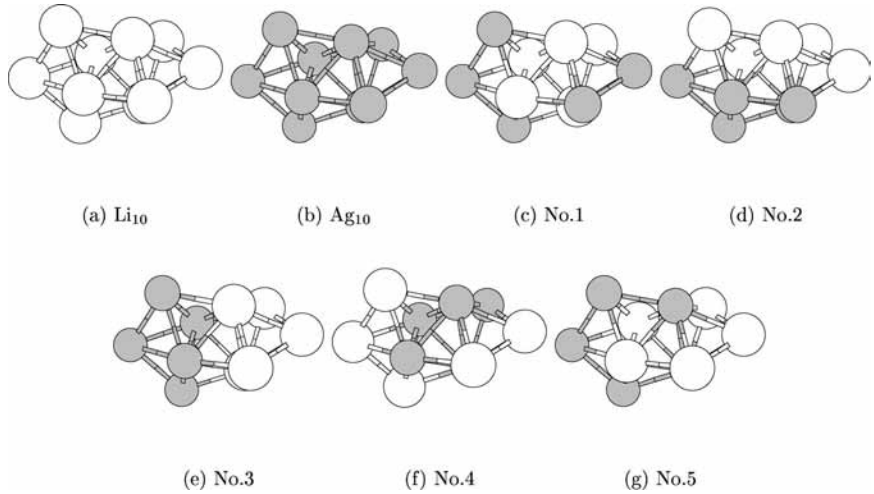

(a) Li_{10} (b) Ag_{10} (c) No.1 (d) No.2

(e) No.3 (f) No.4 (g) No.5

Figure 3. Ag_nLi_{10-n} (n = 0, 5, and 10) homotops obtained by exchanging the positions of silver and lithium atoms based on the same geometry. Lithium atoms are in white.

expected. However, things are quite different when ionic interaction plays an important role as shown by the rest of the graph. Overall, data from SVWN and BP86 are highly correlated with a correlation coefficient of 0.993. On the contrary, SMP gives us the least correlated results with respect to those of BP86. The correlation coefficient is only 0.710, and the slope is off that of SVWN by a lot. By adding the QEq components, we not only improved the correlation coefficient to 0.988, but also bring the slope much more closer to that from SVWN results. Looking at the root-mean-square-errors (RMSE) in Figure 2b, we see that the SMP/QEq dissociation energies are much more consistent with BP86 results than those from the other methods. So we can say that the ionic interaction is essential to calculate D_e of heterodimers and that QEq estimates it well. Surprisingly, as shown in Figure 2a, all potentials give similar results for bond length. This is because the energy curve for ionic interaction has a small slope near the minimum of the nonionic energy curve, so adding the ionic component changes the depth of the energy curve a lot but does not affect the minimum position much.

B. Li and Ag Alloy Clusters. An advantage of SMP/QEq over most empirical potentials is that it includes a crude model of electronic structure and can be used to evaluate ionization energy (IE). In this section, we compared IE calculated with SMP/QEq and with higher level theories, SVWN, B3LYP,[24,25] and BP86. Our sample systems, shown in Figure 3, include five homotops of Ag_5Li_5, which are all based on the same geometry but with different site occupation by the two elements, and pure clusters Ag_{10} and Li_{10}. We calculated the first and second IEs and plotted results in Figure 4, panels a and b. Note that for structure no. 5 we were unable to get BP86 results because of SCF convergence problems. SMP/QEq results follow the trend of values from SVWN well but are consistently higher. On average, SMP/QEq overestimated the first IE by 0.61 eV compared to SVWN, and the overestimation is 1.10 for the second IE. It is quite encouraging that SMP/QEq successfully describes the relative values of IEs, but the systematic overestimation is puzzling. We will go back to this question in section V.D.

As we said in section III, the parameters obtained from the 10-atom ring are better than those from other model systems. This can be seen by looking at the first IE of the Li_5Ag_5 homotops in Figure 3. Using the 12-atom icosahedron parameters, QEq failed to give physically meaningful results for homotops nos. 3, 4, and 5. The IEs calculated for the homotops in Figure 3 are, in order from (a) to (g): 3.98, 6.09, 5.59, 4.71, 4.26, 4.37, and 4.76 eV with the 12-atom cuboctahedron parameters and 4.07, 6.57, 5.63, 4.95, 4.73, 4.59, and 5.01 eV with the 20-atom dodecahedron parameters. Overall, linear regressions show that IEs based on the parameters from the 10-atom ring correlate well with those from SVWN with a correlation coefficient of 0.994, whereas the correlation coefficient is 0.95 for the 20-atom dodecahedron model, and 0.92 for the 12-atom cuboctahedron model. The difference of IE between nos. 3 and 2, and between nos. 3 and 4, is particularly instructive: SVWN (the reference) gives +0.14 and +0.77 eV;

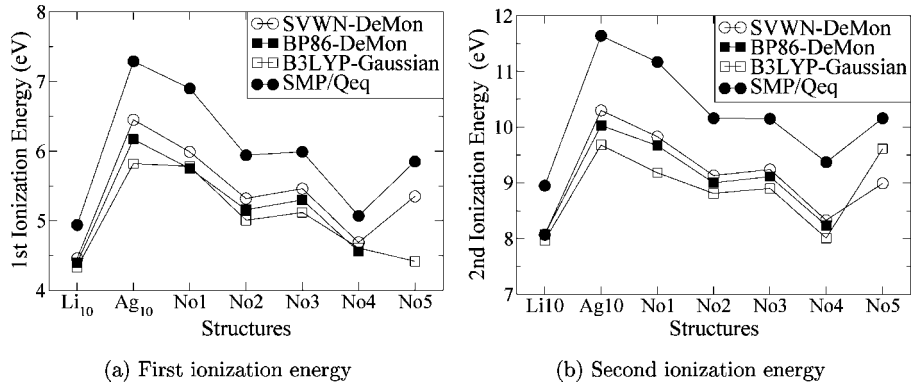

Figure 4. First and second ionization energy of Ag_nLi_{10-n} (n = 0, 5, and 10) isomers shown in Figure 3.

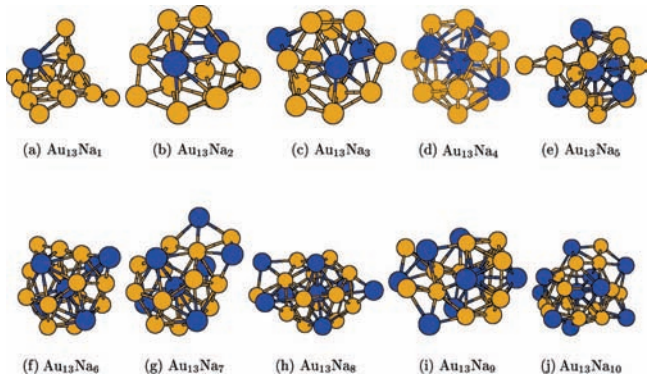

Figure 5. Global minimum of $Au_{13}Na_n$ (n = 1−10) clusters obtained by TSDS with VASP/PBE.

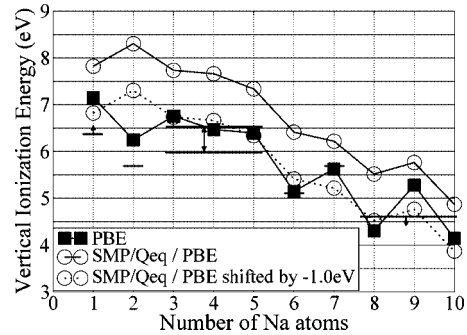

Figure 6. Vertical ionization energy of $Au_{13}Na_n$ (n = 1−10) clusters shown in Figure 5.

TABLE 2: Mixing and Cage-Like Indices of $Au_{13}Na_x$ (x = 1−13) Clusters

x	OMI	LMI	CLI
1	0.179	0.031	0.34
2	0.732	0.052	0.56
3	0.838	0.078	0.64
4	0.768	0.062	0.39
5	0.938	0.056	0.43
6	0.866	0.056	0.40
7	0.898	0.077	0.38
8	0.886	0.081	0.39
9	0.888	0.092	0.49
10	0.976	0.111	0.53

other DFT functionals give results similar to SVWN; QEq parametrized with the 12-atom cuboctahedron gives −0.46 and −0.11 eV; QEq parametrized with the 20-atom dodecahedron gives +0.13 and −0.22 eV; and QEq parametrized with the 10-atom ring gives +0.04 and +0.94 eV. Note also that IEs calculated from QEq are lower when the model structures have higher coordination numbers.

C. Au and Na Alloy Clusters. We performed further test on SMP/QEq's ability to estimate ionization energy because, in our previous test, the sample size is small, only Ag and Li are involved, and we only compared to other theory. Nakajima et al.[19] measured the first IE of $Au_{13}Na_n$, n = 1,10. In order to compare to experiment, we need to find out the structures of these clusters. We did global optimizations by tabu search in descriptor space (TSDS)[18] method. The PBE[28] functional implemented in VASP was used to evaluate energies for optimizations. The global minima (GM) are shown in Figure 5. Three quantities are calculated to show their structural characters and are listed in Table 2. The first one is an overall mixing index (OMI) which represents the mixing of two elements on a large scale. The second one is a local mixing index (LMI) which shows how two elements are mixed locally. The last quantity is a cage-like index (CLI) which is a measure we designed to quantify how much a cluster resembles a cage. Mixing indices are of obvious interest in bimetallic clusters. The CLI is of special interest here because cage structures have been proposed for gold clusters ("golden cages") in a size range from 15 to 20 atoms roughly.[35] We will now briefly explain the OMI, LMI, and CLI. Suppose that we have two kinds of elements A and B in a cluster. We use the symbols d_{AA} and d_{BB} to represent the nearest-neighbor distances for bulk A and B, respectively. Then $d_{AB} = (d_{AA} + d_{BB})/2$ is the estimated A−B bond length. We denote by $\vec{c}_{BA}$ the vector that starts at the center of mass of atoms of B type and ends at the center of mass of atoms of A type: its norm is $||\vec{c}_{BA}||$. We use $P_{B_iA_j}$ to represent the projection of the vector from the ith atom of type B to the jth atom of type A on the direction $\vec{c}_{BA}$, so

$$P_{B_iA_j} = (\vec{r}_{A_j} - \vec{r}_{B_i})\cdot\vec{c}_{BA}/||\vec{c}_{BA}|| \qquad (20)$$

here $\vec{r}_{A_j}$ and $\vec{r}_{B_i}$ are the position vectors of the jth atom of type A and ith atom of type B. By moving all A type atoms together along direction $\vec{c}_{BA}$ until A and B type atoms are completely separated, we can get the displacement, Δ, needed to reach complete separation. Figure 7 gives illustrates this process. Figure 7a is a hypothetical structure; 7b shows what happens to to the position vectors and $\vec{c}_{BA}$ as atoms of A type and B type are pulled apart (Δ is increased); and Figure 7c shows how the projection of vectors $(\vec{r}_{A_j} - \vec{r}_{B_i})$ on the vector $\vec{c}_{AB}$ all become positive at some value of Δ. Choosing a criterion for complete separation is subjective and depends on a given application. We define that A and B type atoms are completely separated when the relation $P_{B_iA_j} \geq d_{AB}/4$ is true for all i and j. We define the OMI as

$$\mathrm{OMI} = \frac{\Delta}{||\vec{c}_{\mathrm{BA}}||+\Delta} \tag{21}$$

To define the LMI, we need three quantities $\bar{s}_{\mathrm{AA}}$, $\bar{s}_{\mathrm{BB}}$, and $\bar{s}_{\mathrm{AB}}$. The variable $\bar{s}_{\mathrm{AA}}$ is a weighted average of the scaled A−A pair distances

$$\bar{s}_{\mathrm{AA}} = \frac{\sum_{i<j} w_{ij} \cdot (||\vec{r}_{\mathrm{A}_i} - \vec{r}_{\mathrm{A}_j}||/d_{\mathrm{AA}})}{\sum_{i<j} w_{ij}} \tag{22}$$

where $w_{ij} = [(||\vec{r}_{\mathrm{A}_i} - \vec{r}_{\mathrm{A}_j}||)/d_{\mathrm{AA}}]^{-4}$, and the sum goes over all A−A pairs. The quantities $\bar{s}_{\mathrm{BB}}$ and $\bar{s}_{\mathrm{AB}}$ are defined in a similar way. We choose a negative power of pair distances as weights to emphasize short bonds in the weighted average. But if we put too much weight on short bonds, the weighted average will be determined only by the shortest pair distance. The power −4 is chosen as a compromise Finally, we have this definition for LMI

$$\mathrm{LMI} = 1 - \frac{\bar{s}_{\mathrm{AB}}}{(a/t)\bar{s}_{\mathrm{AA}} + (b/t)\bar{s}_{\mathrm{BB}}} \tag{23}$$

where a is the number of A−A pairs, b is the number of B−B pairs, and $t = a + b$. We illustrate the meaning of the OMI and LMI with examples of configurations shown in Figure 8. The OMI for Figure 8a−d are 0, 1, 1, and 0, respectively. For Figure 8, panels a, b, and d, LMI < 0 (poor mixing), and for Figure 8c, LMI > 0 (good mixing) because the AB distances are smaller, on average, than the AA or BB distances. Clearly, case 8a (and 8d) is poorly mixed at any scale, and case 8c is well mixed at any scale. Case 8b is well mixed in a global sense (OMI = 1) but poorly mixed in local sense (LMI > 0). The definition of CLI depends on two quantities which we will now explain. Consider an arbitrary point p in a cluster with position $\vec{x}_p$, and denote by d_{ip} the distance between this point and atom i. We define the function f of $\vec{x}_p$: $f(\vec{x}_p) = \min\{d_{ip}$: all i$\}$ Let d_0 be the maximum value of $f(\vec{x}_p)$ among all interior points of the cluster. This d_0 has a geometric interpretation: it is half the length of the longest stick that could be placed at a fixed position in the cluster and could rotate freely in any direction without intersecting any of the nuclei positions. The cube of d_0 (or $4\pi d_0^3/3$) is then a measure of the largest empty space that could be found in the cluster. Another relevant quantity is $d_{\min}$, the smallest interatomic distance in the cluster. The cube of $d_{\min}$ is a way to quantify the volume associated with a missing atom defect in a structure. The CLI is a comparison of these two volumes

$$\mathrm{CLI} = \frac{{d_0}^3}{{d_{\min}}^3} \tag{24}$$

Division by $d_{\min}$ ensures that the same CLI is obtained when a cluster is uniformly expanded. A CLI value greater than one is consistent with this concept of a cage: a continuous empty region of space inside a cluster whose size is clearly bigger than the usual space between atoms. From Table 2, we can observe that all LMIs are bigger than 0. This indicates good local mixing, with $Au_{13}Na_{10}$ having the highest degree of local mixing. Cluster $Au_{13}Na_1$ has an OMI close to zero. This is simply because the only Na atom resides on its surface. The values of OMI being close to one for all other clusters tell us that Au and Na atoms are well mixed on a large scale. Clusters $Au_{13}Na_2$ and $Au_{13}Na_4$ have slightly lower OMIs than other clusters except $Au_{13}Na_1$. By looking at their pictures in Figure 5, we can clearly see that Na atoms really show a tendency to gather on one side of the

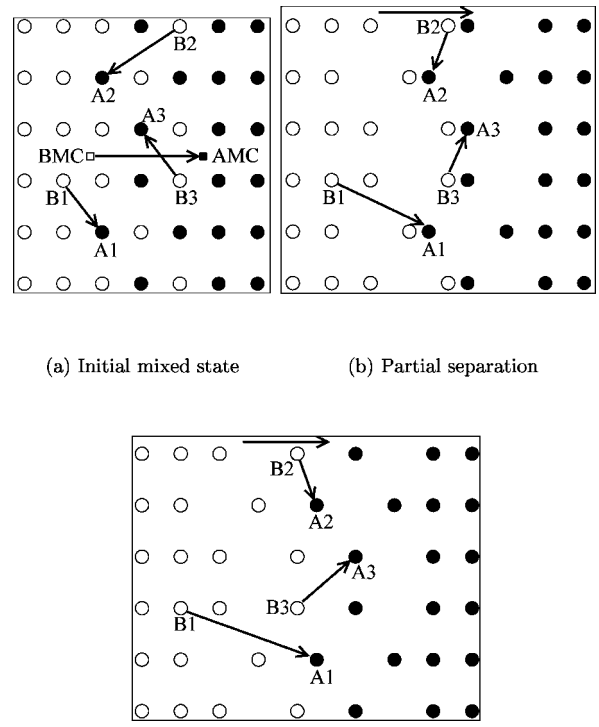

Figure 7. Illustration of how the OMI is calculated. Atoms of A are shown as filled circles, B as open circles. In (a), BMC and AMC are the centers of mass of B-type atoms and A-type atoms, respectively: the vector connecting them is $\vec{c}_{\mathrm{AB}}$.

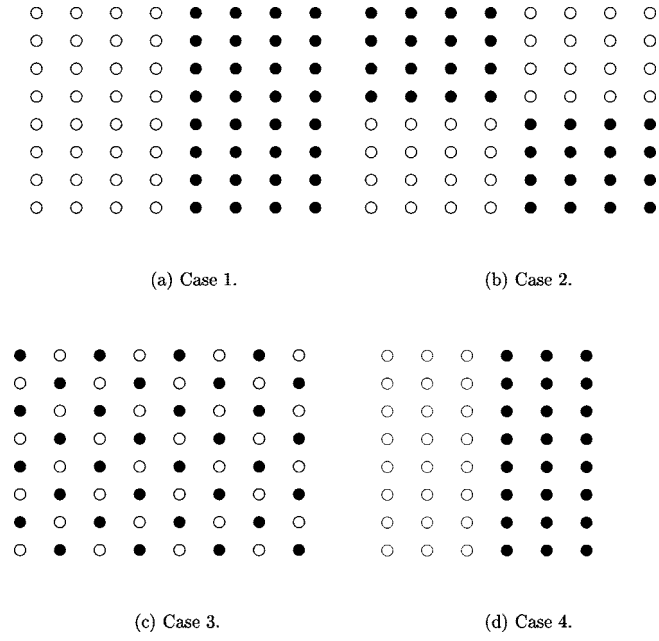

Figure 8. Four types of AB ordering used to illustrate the OMI and LMI: (a) and (d) no overall mixing and poor local mixing; (b) good overall mixing, poor local mixing; (c) good overall mixing and good local mixing.

clusters. Before looking at CLIs of $Au_{13}Na_n$, we want to mention the CLIs of special structures. The CLIs for the 12-atom cuboctahedron (Figure 1b), 12-atom icosahedron (Figure 1c), and 20-atom dodecahedron (Figure 1d) are 1.00, 0.86, and 2.75, respectively. These values are typical of true cages. The CLI of the icosahedron being smaller than 1 reflects the fact that the central atom in a 13-atom icosahedron is slightly compressed. On the other hand, compact structures with no cage feature at all have CLI values in the vicinity of 0.246 (13-atom icosahedron) or 0.230 (13-atom cuboctahedron). If we take the criterion that the 12-atom icosahedron is the smallest possible cage, then structures with CLI smaller than 0.86 are not truly cages. The CLIs in Table 2 show that none of our Au/Na alloy clusters has a cage. Among all clusters, $Au_{13}Na_2$, $Au_{13}Na_3$, and $Au_{13}Na_{10}$ have relatively large CLIs. Figure 5, panels b and c, shows us clearly that $Au_{13}Na_2$ and $Au_{13}Na_3$ do have empty space inside but are simply not large enough to accommodate an atom of a size comparable to a gold atom. It is not easy to visualize empty space in $Au_{13}Na_{10}$ shown in Figure 5j, but when we look closely we see that a part of the cluster is open.

Based on these structures, the first IEs were calculated by SMP/QEq and PBE. Results together with experimental values are shown in Figure 6. The experimental values or ranges are shown by horizontal bars with arrows. The PBE results fall close to experiment except for $Au_{13}Na_2$ and $Au_{13}Na_9$. There are many possible factors that may explain these two mismatches. In experiment, the measurement could relate to isomers other than the GM, so the IE may be an average of different isomers. It is also possible that our global optimization did not reach the true GM. It is an embarrassment in any global optimization that one never knows that the GM was obtained. All we can say is that these structures are the best we could get. Based on the results for these 10 clusters, we still can say that our global optimization generated sensible results and IEs calculated by PBE resemble the experiment. SMP/QEq again gives results consistently higher than those of PBE and experiment. The average overestimation is 1.0 eV as before. If we shift down the SMP/QEq curve by 1.0 eV to make comparison easier (dashed lines in Figure 6), we see that SMP/QEq results agree well with those from PBE and experiments except for $Au_{13}Na_2$ and $Au_{13}Na_7$. There are plenty of possible error sources, particularly the fact that SMP/QEq does not include any quantum effects which could be important for structures with a magic number of electrons (20) like $Au_{13}Na_7$. Adding a correction for electronic shell closing into SMP/QEq might improve it. Another important error source is that our parameters were fitted based on a ring structure which is different from the compact structures of most metal clusters.

D. Systematic Error. As shown in the previous two sections, systematic errors persist in ionization energy calculations. From the fitting precedure described in section III and discussion in section IV, especially eqs 18 and 19, we know that the parameters from a 10-atom ring structure will be good for AIMs in a very similar molecular environment. When we use this set of parameters for compact structures, some errors are expected. We can assess these errors by calculating the first IE for our model systems shown in Figure 1 using parameters from the 10-atom ring and comparing them with those from SVWN. The difference of the first IE from QEq and SVWN, $IE_{QEq} - IE_{SVWN}$, are shown in brackets of Figure 1. For the 10-atom ring itself, the IE from QEq is lower by 0.28 eV which is an error of 4%. For other structures, QEq consistently overestimates the first IE, and for 4 out of 5 structures, the overestimations are around 1 eV. This is consistent with overestimations in previous calculations. Another way to assess the errors is to check the parameters fitted from different model structures. Taking Ag for example, the coefficients from the 10-atom ring are shown in Table 1. Those from the Ag_{12} cuboctahedron, listed starting from the first one, are 4.3306, 3.1165, 0.9682, and 0.9095. When the Ag_{12} cuboctahedron has a +1 charge, the partial charge on each atom is $+^1/_{12}$ independent of parameters. Because the first and second coefficients from the cuboctahedron fit are lower than those from the 10-atom ring, the IE decreases. The QEq calculations overestimate SVWN IE by 0.78 eV or 12% when using the 10-atom ring parameters and underestimate by 0.19 eV or 3% when using the 12-atom cuboctahedron parameters. We did similar tests on other elements and found the above argument is true for all elements and all model structures we have. As shown in eq 19, all parameters are environment dependent. That is, if atoms of the same element are in different molecular environment in one molecule, they are actually different AIMs. Ideally we should assign different parameters to each of them. We think such a scheme would remove systematic errors. Another advantage of that scheme is that we could estimate charge distributions and dipole moments in pure clusters. However putting this idea into practice is not easy and will require robust automated procedures to derive parameters for AIMs representative of various environments.

VI. Conclusion

Based on the analysis and calculations of this study, we can say that the inclusion of third and fourth order terms in the energy expansion eq 1, and use of self-consistent screened Coulomb interactions J_{ii} in eq 7 eliminate the problem of unphysical atomic charges. It makes QEq more reliable and potentially more accurate. Results for metal dimers and 55-atom alloy clusters[1] show that the QEq ionic contributions to the total energy are essential in mixed metal systems when there are appreciable electronegativity differences between atoms. The IEs of Ag_5Li_5 and $Au_{13}Na_n$ ($n = 1-10$) calculated by QEq are surprisingly good, especially in a relative sense (trends). This is important because the IE is one of the easiest property to measure and IEs of metal clusters have been found to correlate with chemical reactivity.[36] More importantly, the analysis in section IV establishes a connection between DFT and the SMP/QEq approximation. This gives insight into the validity of the approximations and ways to improve them. In particular, we made the assumption, in our current implementation of SMP/QEq, that the last two terms of eq 14 do not change appreciably when we go from a neutral to a charged system. This may be approximately true in large metal clusters where charging involves the filling or emptying of mostly nonbonding orbitals, but it is clearly a bad approximation in small systems, or covalently bonded systems, where charging occurs via the filling or emptying of bonding and antibonding orbitals. An extreme example of this would be $He_2/He_2^+/He_2^{2+}$. Therefore, an important improvement in the future will be to model the charge-dependent changes to the covalent energy terms, in both the parametrization and application stages of SMP/QEq.

Acknowledgment. This work was made possible by the facilities of the Shared Hierarchical Academic Research Computing Network (SHARCNET:www.sharcnet.ca).

References and Notes

(1) Zhang, M.; Fournier, R. *J. Mol. Struct.: THEOCHEM* **2006**, *762*, 49.

(2) Cieplak, P.; Cornell, W. D.; Bayly, C.; Kollman, P. A. *J. Comput. Chem.* **1995**, *16*, 1357.

(3) Sanderson, R. T. *Science* **1951**, *114*, 670.

(4) Sanderson R. T. *Chemical Bonds and Bond Energy*, 2nd ed.; Academic Press: New York, 1976.
(5) Mortier, W. J.; Ghosh, S. K.; Shankar, S. *J. Am. Chem. Soc.* **1986**, *108*, 4315.
(6) Mortier, W. J.; Van Genechten, K.; Gasteiger, J. *J. Am. Chem. Soc.* **1985**, *107*, 829.
(7) Bultinck, P.; Langenaeker, W.; Lahorte, P.; De Proft, F.; Geerlings, P.; Waroquier, M.; Tollenaere, J. P. *J. Phys. Chem. A* **2002**, *106*, 7887.
(8) Bultinck, P.; Langenaeker, W.; Lahorte, P.; De Proft, F.; Geerlings, P.; Waroquier, M.; Tollenaere, J. P.; Van Alsenoy, C.; Tollenaere, J. P. *J. Phys. Chem. A* **2002**, *106*, 7895.
(9) York, D. M.; Yang, W. *J. Chem. Phys.* **1996**, *104*, 159.
(10) Louwen, J. N.; Vogt, E. T. C. *J. Mol. Catal. A* **1998**, *134*, 63.
(11) Njo, S. L.; Fan, J.; van de Graaf, B. *J. Mol. Catal. A* **1998**, *134*, 79.
(12) Fournier R.; Zhang M.; Soudagar Y.; Hopkinson M. *Lecture Series on Computers and Computational Sciences*; Simos, T. E., Maroulis, G., Eds.; VSP Brill Academic Publishers: Utreche, The Netherlands, 2005; Vol. 3, p 51.
(13) Rappé, A. K.; Goddard, W. A., III. *J. Phys. Chem.* **1991**, *95*, 3358.
(14) Kitao, O.; Ogawa, T. *Mol. Phys.* **2003**, *101*, 3.
(15) Ogawa, T.; Kitao, O.; Kurita, N.; Sekino, H. *Chem-Bio Informat. J.* **2003**, *3*, 78.
(16) Iczkowski, R. P.; Margrave, J. L. *J. Am. Chem. Soc.* **1961**, *83*, 3547.
(17) Parr R. G.; Yang W. *Density-Functional Theory of Atoms and Molecules*; Oxford University Press: New York, 1989.
(18) Cheng, J.; Fournier, R. *Theor. Chem. Acc.* **2004**, *112*, 7.
(19) Nakajima, A.; Hoshino, K.; Naganuma, T.; Watanabe, K.; Kaya, K. *Z. Phys. D* **1993**, *26*, S 89.
(20) Vosko, S. H.; Wilk, L.; Nusair, M. *Can. J. Phys.* **1980**, *58*, 1200.
(21) Hohenberg, P.; Kohn, W. *Phys. Rev. B* **1964**, *136*, 864.
(22) Kohn, W.; Sham, L. J. *Phys. Rev. A* **1965**, *140*, 1133.
(23) Slater J. C. *Quantum Theory of Molecules and Solids. Vol. 4: The Self-Consistent Field for Molecules and Solids*; McGraw-Hill: New York, 1974.
(24) Becke, A. D. *J. Chem. Phys.* **1993**, *98*, 5648.
(25) Lee, C.; Yang, W.; Parr, R. G. *Phys. Rev. B* **1988**, *37*, 785.
(26) Becke, A. D. *Phys. Rev. A* **1988**, *38*, 3098.
(27) Perdew, J. P. *Phys. Rev. B* **1986**, *33*, 8822.
(28) Perdew, J. P.; Burke, K.; Ernzerhof, M. *Phys. Rev. Lett.* **1996**, *77*, 3865.
(29) Bader R. F. W. *Atoms in Molecules. A Quantum Theory*; Oxford University Press: New York, 1990.
(30) Bader, R. F. W.; Nguyen-Dang, T. T. *Adv. Quantum Chem.* **1981**, *14*, 63.
(31) Zhou, X. W.; Wadley, H. N. G. *J. Phys.: Condens. Matter* **2005**, *17*, 3619.
(32) Demiralp, E.; Çagin, T.; Goddard III, W. A. *Phys. Rev. Lett.* **1999**, *82*, 1708.
(33) (a) St-Amant, A.; Salahub, D. R. *Chem. Phys. Lett.* **1990**, *169*, 387. (b) St-Amant A. 1992, Ph.D. Thesis, University of Montreal. ; Casida M. E.; Daul C.; Goursot A.; Koester A.; Pettersson L. G. M.; Proynov E.; St-Amant A.; Salahub D. R. (principal authors) and Chrétien S.; Duarte H.; Godbout N.; Guan J.; Jamorski C.; Leboeuf M.; Malkin V.; Malkina O.; Nyberg M.; Pedocchi L.; Sim F.; Vela A. (contributing authors) 1998, deMon-KS software version 3.2.
(34) Andzelm, J.; Radzio, E.; Salahub, D. R. *J. Chem. Phys.* **1985**, *83*, 4573.
(35) Bulusu, S.; Wang, L. S.; Zeng, X. C. *Proc. Natl. Acad. Sci.* **2006**, *103*, 8326.
(36) Knickelbein, M. B. *Annu. Rev. Phys. Chem.* **1999**, *50*, 79.

JP8063273